



CHORUS

This is the accepted manuscript made available via CHORUS. The article has been published as:

Unified explanation of chemical ordering, the Slater-Pauling rule, and half-metallicity in full Heusler compounds

Sergey V. Faleev, Yari Ferrante, Jaewoo Jeong, Mahesh G. Samant, Barbara Jones, and
Stuart S. P. Parkin

Phys. Rev. B **95**, 045140 — Published 26 January 2017

DOI: [10.1103/PhysRevB.95.045140](https://doi.org/10.1103/PhysRevB.95.045140)

A unified explanation of chemical ordering, the Slater-Pauling rule, and half-metallicity in full Heusler compounds.

Sergey V. Faleev,^{1,*} Yari Ferrante,^{1,2,3} Jaewoo Jeong,¹ Mahesh G. Samant,¹ Barbara Jones,¹ and Stuart S. P. Parkin^{1,3,†}

¹IBM Research - Almaden, 650 Harry Road, San Jose, California 95120, USA

²Martin Luther University, 06099 Halle (Saale), Germany

³Max Planck Institute for Microstructure Physics, 06120 Halle (Saale), Germany

(Dated: December 6, 2016)

In the present work we developed an orbital coupling model for cubic full Heusler compounds that provides a *unified* set of rules that account for the chemical ordering, magnetic moment and the composition of the most promising candidates for half-metallicity. Origin and limitations of the rules are clearly described. To the best of our knowledge all several dozens known in literature half-metallic Heusler compounds that follow the $M_t = N_t - 24$ or $M_t = N_t - 28$ generalized Slater-Pauling behaviour satisfy derived half-metallicity rule. Calculations performed by using the density functional theory (DFT) - performed for 259 compounds - confirm the validity of our model and derived rules for broad classes of Heusler compounds.

PACS numbers: 85.75.-d

I. I. INTRODUCTION

Heusler compounds X_2YZ where X and Y are transition-metal elements and Z is a main group element have been intensively studied, both theoretically and experimentally, for their potential applications in spintronics, energy and magnetocaloric technologies¹. Due to flexibility in composition Heusler compounds can be realised as high-temperature ferri- and ferromagnets², multiferroic shape-memory alloys³, and topological insulators^{4,5}. Current interest in spintronic applications of Heuslers arises largely from the observation of half-metallicity in some of them⁶ giving rise to giant tunneling magnetoresistance at room temperature⁷.

Despite increasing interest in Heuslers there is still a lack of fundamental understanding regarding the nature of chemical ordering in these materials. Researchers have to rely on empirical rules⁸⁻¹⁰ for chemical ordering without clear understanding of the origin and limitations of these rules. Moreover, as we show below, the conventional explanation of half-metallicity in Heusler compounds^{11,12} is incomplete, with incorrect symmetry assignments. In the present paper we present a model for orbital coupling that gives a *unified* explanation of chemical ordering, the Slater-Pauling rule and composition rule for the most promising half-metallic Heusler compounds. The validity of the model and derived rules are supported by DFT calculations performed for 259 Heusler compounds.

II. II. ORBITAL COUPLING MODEL

A. A. Orbital coupling in regular Heusler compounds for states at the Γ and X symmetry points

Crystal structure of cubic Heusler compound is shown in Fig. 1(a) with four sites forming four fcc sublattices: site Z (occupied by atom Z), site II, octahedrally coordinated by Z, and sites I and I', tetrahedrally coordinated by Z. Equivalent sites I and I' can be occupied by two X atoms (regular structure), or by one X atom and one Y atom (inverse structure). Our orbital coupling model for cubic Heusler compounds includes 18 orbitals $\phi_i(\mathbf{r})$ ($i = 1, \dots, 18$): 3 p -orbitals on site Z and 15 d -orbitals on sites I, I', and II. We will use linear combinations of orbitals on sites I and I': $d^{(\pm)}(I) \equiv d(I) \pm d(I')$ rather than $d(I)$ and $d(I')$. Transformation to reciprocal space is performed as $\phi_{\mathbf{k},i}(\mathbf{r}) = \sum_{\mathbf{T}} e^{i\mathbf{k}\cdot\mathbf{T}} \phi_i(\mathbf{r} - \mathbf{T})$, where the summation is taken over all translation vectors of the fcc lattice. Below we consider the coupling between these 18 orbitals for states of regular Heusler compound at the Γ and X symmetry points.

Due to the symmetry of regular Heusler structures there are only 8 non-zero non-diagonal Hamiltonian matrix elements $\langle \phi_{\mathbf{k},i} | H | \phi_{\mathbf{k},j} \rangle$ at the Γ -point ($\mathbf{k} = 0$): three $\langle p_\alpha(Z) | H | d_{\beta\gamma}^{(-)}(I) \rangle$ matrix elements with $\{\alpha; \beta\gamma\} = \{x; yz\}, \{y; xz\}, \{z; xy\}$, and five $\langle d_{\alpha\beta}(II) | H | d_{\alpha\beta}^{(+)}(I) \rangle$ matrix elements with $\alpha\beta = xx, zz, xy, xz, yz$.

We use Co_2MnGe as an example of regular Heusler compound for illustration of our model. The minority bands of regular Co_2MnGe are shown in Fig 1(c). Here and below bands are colorized according to the weights of the d -orbitals on sites I and I' (red), weight of the d -orbitals on site II (green), and the weight of all the other orbitals (blue). In Fig 1(c) we label 15 minority states at the Γ -point by Roman numerals, from (i) to (xv). The

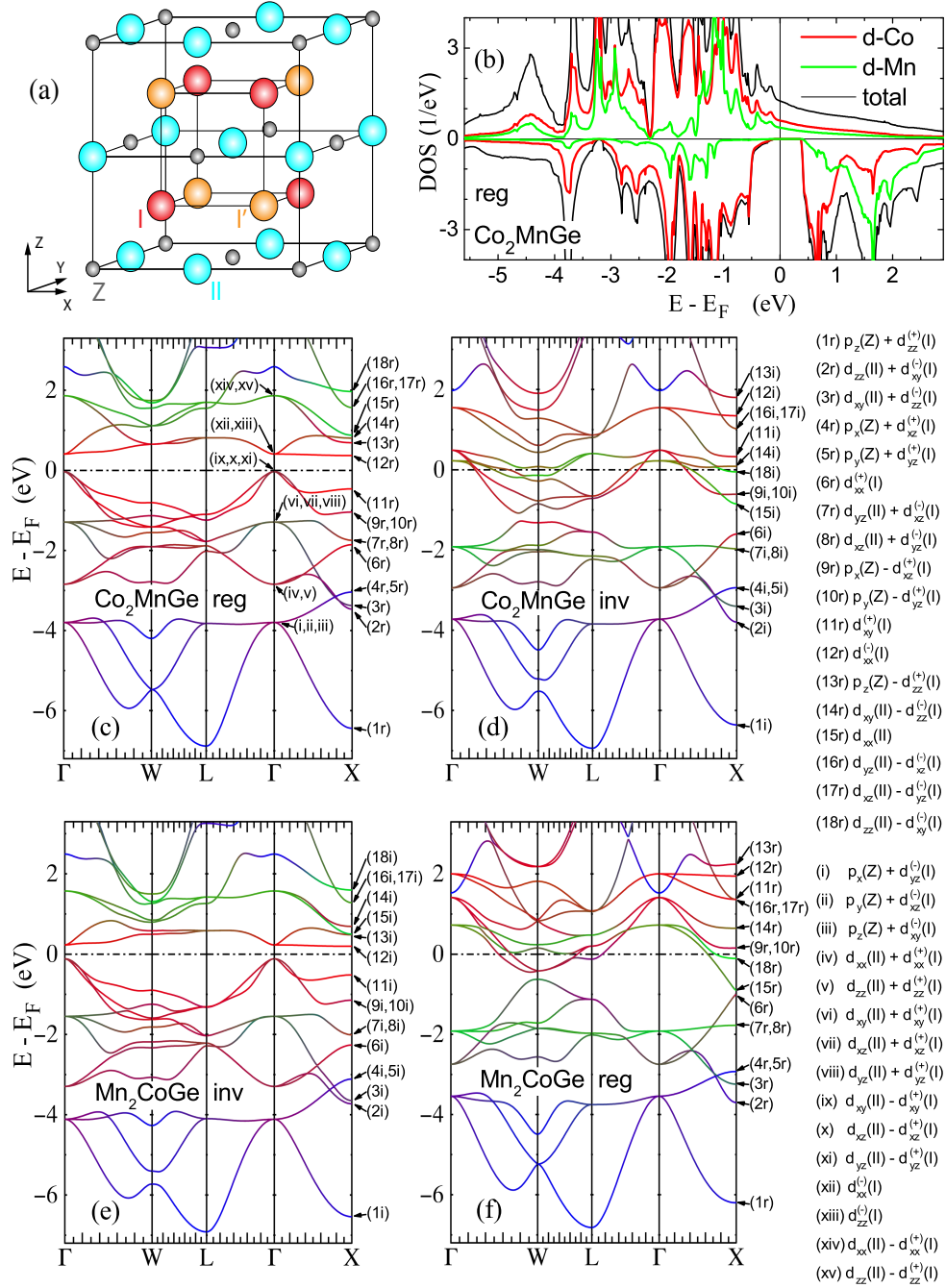


FIG. 1: (Color online). (a) crystal structure of cubic Heusler compound, (b) DOS for majority ($DOS > 0$) and minority ($DOS < 0$) bands of regular Co_2MnGe . Minority bands of regular (c) and inverse (d) Co_2MnGe and inverse (e) and regular (f) Mn_2CoGe . See text for details.

orbital composition of these states derived from non-zero Hamiltonian matrix elements described above is shown at the bottom right of Fig 1, where the sign '+' or '-' between the orbitals denotes bonding or antibonding hybridisation of the orbitals. Three remaining states derived from the 18-orbital coupling model at the Γ -point, that we label as (xvi),(xvii), and (xviii) have the orbital composition $p_x(Z) - d_{yz}^{(-)}(I)$, $p_y(Z) - d_{xz}^{(-)}(I)$, and $p_z(Z) - d_{xy}^{(-)}(I)$,

correspondingly. The energy of these states, $E_F + 3.73$ eV, is above the top edge of the Fig. 1 (c). [Note that two s -character states with energies $E_F - 12$ eV and $E_F + 2.59$ eV at Γ -point are not included in our model.]

In the orbital coupling scheme proposed in¹¹ the states (ix,x,xi) of Co_2MnGe at Γ -point are incorrectly identified as being composed of $d_{\alpha\beta}^{(-)}(I)$ orbitals ($\alpha\beta = xy, xz, yz$) instead of $d_{\alpha\beta}(II) - d_{\alpha\beta}^{(+)}(I)$. Our calculations show that

(ix,x,xi) states at Γ -point have 19% weight from d -orbitals of Mn, which disagrees with assumption¹¹ that these states are non-bonding to Mn. Description of the orbital identification, including specific weights of each orbital, for states from (i) to (xviii) is presented in Supplemental Material at URL-inserted-by-publisher.

At the X-point, $\mathbf{k} = (0, 0, 2\pi/a)$ [a is the lattice constant] the $\phi_i(\mathbf{r} - \mathbf{T})$ orbitals in the sum $\phi_{\mathbf{k},i}(\mathbf{r}) = \sum_{\mathbf{T}} e^{i\mathbf{k}\mathbf{T}} \phi_i(\mathbf{r} - \mathbf{T})$ have alternating signs $e^{i\mathbf{k}\mathbf{T}} = \pm 1$ for \mathbf{T} in alternating xy -planes. Due to the symmetry of regular Heusler structures there are only 7 non-zero non-diagonal Hamiltonian matrix elements $\langle \phi_{\mathbf{k},i} | H | \phi_{\mathbf{k},j} \rangle$ at the X-point: three $\langle p_\alpha(Z) | H | d_{\alpha\beta}^{(+)}(I) \rangle$ with $\alpha\beta = xz, yz, zz$ and four $\langle d_{\alpha\beta}(II) | H | d_{\gamma\delta}^{(-)}(I) \rangle$ with $\{\alpha\beta; \gamma\delta\} = \{zz; xy\}, \{xy; zz\}, \{yz; xz\}, \{xz; yz\}$.

In Fig 1(c) we label 18 states at X-point from (1r) to (18r) ['r' refers to 'regular']: orbital composition for these states derived from non-zero Hamiltonian matrix elements described above is shown at the right of Fig 1. Description of the orbital identification for states from (1r) to (18r) is presented in Supplemental Material.

Tables I and II in Supplemental Material confirm that 18 considered minority states of Co_2MnGe at both the Γ and X points have either nonzero *or zero* weights from 18 spherical harmonics (orbitals) included in our model in agreement with the orbital compositions listed in Fig. 1. In addition, these tables show that the weights of spherical harmonics not included into the 18-orbital model as well as contributions from the interstitial regions are small for these states, therefore confirming the validity of our model for description of states in vicinity of the Fermi energy in Heusler compounds.

B. Energy ordering of minority states of regular Co_2MnGe at Γ and X symmetry points

The bonding-antibonding gap between states (vi,vii,viii) and (ix,x,xi) of Co_2MnGe at the Γ point is smaller compared to that between states (iv,v) and (xiv,xv) since, as seen by colors of these states, antibonding states (ix,x,xi) [(xiv,xv)] have larger [smaller] weights from heavier Co while bonding states (vi,vii,viii) [(iv,v)] have larger [smaller] weights from lighter Mn. States (xii,xiii) (non-bonding to sites Z and II) are strongly localized and therefore have large exchange splitting energy that pushes them above the Fermi energy, E_F , forming a band-gap.

The energy ordering of (1r-18r) states of Co_2MnGe at X point can be deduced from general considerations. States (1r,4r,5r) mostly consist of $p(Z)$ orbitals and thus have low energy. States (2r,3r,7r,8r) and (14r,16r,17r,18r) are bonding and antibonding hybridisation of $d(II)$ and $d^{(-)}(I)$ orbitals that have large bonding-antibonding gap since sites I and II are the nearest neighbours with strong orbital interaction. State (15r) is composed of sole $d_{xx}(II)$ orbital with energy determined by the valence of the atom

on site II. As will be shown below the fact that this state is localized on site II is important for derivation of the rule for composition of compounds that are more or less likely to be half-metallic (the 'half-metallicity' rule).

Energy ordering of states (6r,9r,10r,11r,12r,13r) is determined by overlaps of d -orbitals on sites I and I' , which are the second nearest neighbours. State (6r) has lowest energy in this series due to strong 'lobes-favorable' $I - I'$ interaction (lobes of orbitals point to each other) with bonding along both x and y axes. States (9r,10r) have higher energy than (6r) due to weaker 'lobes-unfavorable' $I - I'$ interaction (lobes do not point to each other) with bonding along z and antibonding along x or y axes [$p(Z)$ weight is small for these states, see Supplemental Material]. State (11r) has higher energy than (9r,10r) since similar 'lobes-unfavorable' antibonding occurs now along both x and y axes. State (12r) has higher energy than (11r) since strong 'lobes-favorable' antibonding occurs along both x and y axes. Thus, the difference in strength of the $I-I'$ coupling for $d_{xy}^{(+)}(I)$ and $d_{xx}^{(-)}(I)$ orbitals leads to the band gap at the X-point. State (13r) has higher energy than (12r) since strong 'lobes-favorable' antibonding occurs along z axis with additional push-up from antibonding with $p(Z)$.

States (11r) and (12r) do not couple to Z and II sites and, therefore, are strongly localized, leading to flat bands near the X-point [see Fig 1(c)]. Thus, the Co pDOS increases at $E_F - 0.5\text{eV}$ and $E_F + 0.4\text{eV}$, without increase of the Mn pDOS [see Fig 1(b)]. Since states (9r-13r) at X-point and states (xii,xiii) at Γ -point do not couple to Mn, the minority pDOS of Mn in the energy window ($E_F - 1\text{eV}, E_F + 0.5\text{eV}$) is small. As will be discussed below, small minority pDOS of Y atom at site II in a broad energy window near E_F is a general feature of regular Heusler compounds with X=Mn,Fe,Co and Y atom with lower valence than X [see Fig. 3 (a),(c),(e)].

C. Orbital coupling in inverse Heusler compounds

Let us now consider the orbital coupling in inverse Heusler compounds. Since sites I and I' are now occupied by different atoms, for every non-zero non-diagonal Hamiltonian matrix element with $d^{(+)}(I)$ [$d^{(-)}(I)$] orbital in the regular compound, there is a similar nonzero matrix element with $d^{(-)}(I)$ [$d^{(+)}(I)$] orbital in the inverse compound. Thus, the number of non-zero, non-diagonal matrix elements at Γ or X points doubles as compared to the regular compound. On the other hand, these additional matrix elements have contributions from sites I and I' with opposite signs [these contributions exactly cancel each other when sites I and I' are occupied by the same type of atoms]. Therefore, these additional matrix elements can be treated as small corrections (at least when valences of X and Y atoms are not very different) and, in first approximation, the site-orbital composition of bands in the inverse Heusler compounds can be considered as

the same as in the regular compounds. We label states of the inverse compound at the X-point that have (mostly) the same site-orbital composition as the (1r-18r) states of regular compound as (1i-18i) ['i' refers to 'inverse'], assuming that corrections arising from additional matrix elements are small.

D. Slater-Pauling rule

When there is a minority band-gap and E_F lies within this gap, the magnetic moment, M_t (in μ_B), of the Heusler compound is given by the Slater-Pauling rule^{11,13}: $M_t = N_t - 24$, where N_t is total number of valence electrons per formula unit. This rule follows from counting the occupied minority bands, which equals 12 [including the s -band at $E_F - 12\text{eV}$ in Co_2MnGe]. In many compounds the minority band-gap does not exist, but the Slater-Pauling rule is still approximately valid since minority DOS between (11r/i) and (12r/i) bands at the X point usually has a valley (we will refer to this as the 'SP valley') with E_F within this valley. Since E_F within the SP valley lowers the total energy, the majority bands shift so as to be populated by exactly $N_t - 12$ electrons, if there is a minority band-gap, and approximately so in the absence of a band-gap. This is an important point that allows the formulation of rules, discussed herein, that only depend on the minority states.

III. CHEMICAL ORDERING IN CUBIC HEUSLER COMPOUNDS

A. Chemical ordering in Co_2MnGe and Mn_2CoGe

Minority bands of inverse Co_2MnGe are shown in Fig 1(d) with the orbital compositions identified at the X-point as discussed above. Note that, since the d_{xx} orbitals are not part of any non-zero, non-diagonal Hamiltonian matrix elements in the regular structure, the states (6i,12i,15i) are composed solely of d_{xx} orbitals analogously to the states (6r,12r,15r). One can see in Fig 1(d) that the energy of the red/reddish bands composed of orbitals on sites I and I' (one of these sites is now occupied by lighter Mn atom) generally increase, while the energy of green/greenish bands composed of orbitals on site II (occupied now by heavier Co atom) generally decrease as compared to the bands of regular Co_2MnGe shown in Fig 1(c). In particular, the unoccupied (green) state (15r) becomes an occupied state (15i), while the occupied (red) state (11r) becomes an unoccupied state (11i). The rise of red bands and fall of green bands leads to closure of the band-gap with significant DOS near E_F . The increase of the DOS near E_F leads to an increase of the total energy of inverse Co_2MnGe as compared to regular Co_2MnGe by 0.88 eV (see Table I).

Let us now consider inverse Mn_2CoGe . Note that our description of energy ordering and orbital composition of the bands was site-based and the only atom-dependent information that was used was as to which atom is heavier. Therefore, the site-orbital composition and ordering of bands in inverse Mn_2CoGe and regular Co_2MnGe should be similar (both compounds have light Mn atom on site II). As seen in Fig 1(e) the minority bands of inverse Mn_2CoGe are indeed very similar to the minority bands of regular Co_2MnGe . In regular Mn_2CoGe , when heavier Co atom switches from site I to site II, the energy of the green [red] bands decreases [increases] as compared to the bands of inverse Mn_2CoGe [see Fig 1(e),(f)]. Analogously to the inverse Co_2MnGe case, in regular Mn_2CoGe the band-gap closes and the DOS near E_F increases, resulting in an increase of the total energy by 0.57 eV (see Table I).

B. The 'lightest atom' rule for chemical ordering in cubic Heusler compounds

Note that the conclusion about the stability of regular Co_2MnGe and inverse Mn_2CoGe derived above was based solely on geometrical analysis of orbital overlaps and consideration which atom, X or Y, has smaller number of valence electrons, N . From these examples we can derive a general rule - the 'lightest atom' rule - that states that the cubic Heusler compound X_2YZ is stable in whichever phase (regular or inverse) in which site II is occupied by the 'lightest atom' - the lower-valence atom or atom with smaller atomic number if $N(X) = N(Y)$. This rule follows from the fact that at the X-point the energy of the highest occupied bands (9-11r/i), all of which are non-bonding to site II, increases when the lower-valence atom switches from site II to site I, thereby, leading to a closure of the SP valley (and the minority band-gap if there is one) and consequently a larger DOS near E_F and, therefore, a larger total energy.

The preference of the lower-valence atom to occupy site II in Heusler compounds has been recognized for almost a decade^{8,9,14}, but it was only known as an 'empirical rule of thumb'¹⁰ since there was no clear understanding of its origin. The limitation of the 'lightest atom' rule is that it cannot be applied to heavier compounds where (11r/i) band is pushed far below E_F and flat (12r/i) band crosses E_F resulting in peaky structure of minority DOS near E_F . With large DOS at E_F one cannot make a conclusion as to which cubic phase is more stable (in such case the tetragonal phase is often more stable than cubic¹⁵).

C. Results of calculations for broad classes of Heusler compounds that support the 'lightest atom' rule

To support our explanation of the 'lightest atom' rule and clarify its range of validity we performed DFT cal-

TABLE I: Calculated lattice constant a_r (a_i) and total magnetic moment m_r (m_i) per formula unit for regular (inverse) phase and the total energy difference, ΔE , between the phase where the lower-valence (or lower atomic number if the valence is the same) atom does not and where it does occupy site II, are presented for 259 Heusler compounds. Note that ΔE is positive if the 'lightest atom' rule is satisfied. The magnetic moment of the half metallic compounds that satisfy the Slater-Pauling rule are highlighted in red, and the magnetic moment of compounds that satisfy the Slater-Pauling rule with $dM \equiv |M_t - (N_t - 24)| < 0.5$ accuracy are highlighted in green. Chemical formula of compounds that are predicted to have inverse structure by the 'lightest atom' rule are highlighted in blue.

	a_r	m_r	a_i	m_i	ΔE		a_r	m_r	a_i	m_i	ΔE		a_r	m_r	a_i	m_i	ΔE		a_r	m_r	a_i	m_i	ΔE
	(Å)	(μ_B)	(Å)	(μ_B)	(eV)		(Å)	(μ_B)	(Å)	(μ_B)	(eV)		(Å)	(μ_B)	(Å)	(μ_B)	(eV)		(Å)	(μ_B)	(Å)	(μ_B)	(eV)
Mn ₂ FeAl	4.14	7.07	4.06	1.00	0.30	Fe ₂ MnAl	4.01	2.00	4.05	1.93	0.25	Co ₂ MnAl	4.03	4.01	4.07	5.25	0.83	Ru ₂ MnGa	4.23	2.13	4.27	4.00	1.40
Mn ₂ CoAl	4.16	7.44	4.06	2.00	0.52	Fe ₂ CoAl	4.06	5.58	4.03	4.96	0.46	Co ₂ FeAl	4.03	4.98	4.02	4.39	0.69	Ru ₂ FeGa	4.24	3.14	4.26	3.21	0.95
Mn ₂ NiAl	4.16	0.00	4.11	1.15	0.54	Fe ₂ NiAl	4.06	4.36	4.06	4.78	0.73	Co ₂ NiAl	4.01	2.50	4.02	2.97	0.07	Ru ₂ CoGa	4.21	1.48	4.24	2.74	-0.32
Mn ₂ CuAl	4.21	0.00	4.16	0.15	0.34	Fe ₂ CuAl	4.10	3.99	4.10	4.17	0.43	Co ₂ CuAl	4.02	1.20	4.06	2.56	-0.01	Ru ₂ MnIn	4.40	2.19	4.45	4.72	0.92
Mn ₂ FeGa	4.15	7.19	4.09	1.02	0.18	Fe ₂ MnGa	4.02	2.02	4.13	7.22	0.07	Co ₂ MnGa	4.05	4.08	4.09	5.38	0.69	Ru ₂ FeIn	4.40	3.25	4.41	3.78	0.61
Mn ₂ CoGa	4.18	7.77	4.08	2.00	0.33	Fe ₂ CoGa	4.08	5.97	4.05	5.11	0.40	Co ₂ FeGa	4.04	5.00	4.05	4.80	0.63	Ru ₂ CoIn	4.40	3.43	4.40	3.68	0.05
Mn ₂ NiGa	4.16	0.00	4.13	1.16	0.31	Fe ₂ NiGa	4.08	4.63	4.07	4.86	0.59	Co ₂ NiGa	4.02	2.62	4.03	2.99	0.01	Ru ₂ MnGe	4.25	3.03	4.23	1.34	1.74
Mn ₂ CuGa	4.23	0.00	4.20	0.30	0.13	Fe ₂ CuGa	4.13	4.45	4.12	4.41	0.28	Co ₂ CuGa	4.04	1.19	4.07	2.63	-0.05	Ru ₂ FeGe	4.24	3.96	4.25	3.18	1.22
Mn ₂ FeSi	3.96	2.09	3.96	2.00	0.38	Fe ₂ MnSi	3.95	3.00	3.95	3.03	0.24	Co ₂ MnSi	3.98	5.00	3.97	4.18	0.88	Ru ₂ CoGe	4.21	1.96	4.25	2.84	-0.80
Mn ₂ CoSi	4.03	6.28	3.97	3.00	0.73	Fe ₂ CoSi	3.95	4.35	3.96	4.93	0.56	Co ₂ FeSi	3.98	5.46	3.95	3.96	0.38	Ru ₂ MnSn	4.41	3.07	4.44	4.34	1.39
Mn ₂ NiSi	4.02	-0.11	4.02	1.07	0.27	Fe ₂ NiSi	3.95	3.18	3.99	4.68	0.31	Co ₂ NiSi	3.94	2.04	3.95	2.38	-0.19	Ru ₂ FeSn	4.40	4.13	4.41	3.94	1.04
Mn ₂ CuSi	4.06	4.43	4.07	1.00	0.03	Fe ₂ CuSi	3.98	2.50	4.02	3.71	-0.02	Co ₂ CuSi	3.94	0.00	3.99	2.38	-0.68	Ru ₂ CoSn	4.38	3.05	4.40	3.69	-0.39
Mn ₂ FeGe	4.04	1.98	4.05	2.00	0.41	Fe ₂ MnGe	4.02	3.00	4.08	5.98	0.21	Co ₂ MnGe	4.06	5.00	4.06	4.61	0.88	Ru ₂ MnSb	4.41	4.01	4.45	4.48	1.64
Mn ₂ CoGe	4.11	6.47	4.06	3.00	0.57	Fe ₂ CoGe	4.05	5.22	4.04	5.05	0.54	Co ₂ FeGe	4.06	5.63	4.03	4.23	0.44	Ru ₂ FeSb	4.40	4.37	4.40	3.79	1.09
Mn ₂ NiGe	4.14	-0.01	4.13	0.88	0.22	Fe ₂ NiGe	4.05	3.89	4.08	5.06	0.36	Co ₂ NiGe	4.02	2.41	4.05	2.58	-0.18	Ru ₂ CoSb	4.37	2.82	4.40	3.48	-0.79
Mn ₂ CuGe	4.15	4.64	4.20	0.63	0.12	Fe ₂ CuGe	4.08	3.55	4.11	4.36	0.08	Co ₂ CuGe	4.02	0.01	4.08	2.62	-0.55	Rh ₂ MnGa	4.28	4.09	4.33	4.02	1.54
Mn ₂ FeSn	4.34	8.03	4.27	2.00	0.12	Fe ₂ MnSn	4.25	5.82	4.31	7.57	-0.05	Co ₂ MnSn	4.23	5.01	4.27	5.63	0.97	Rh ₂ FeGa	4.27	4.27	4.28	3.08	1.30
Mn ₂ CoSn	4.38	8.44	4.30	1.49	0.30	Fe ₂ CoSn	4.26	6.00	4.23	5.41	0.57	Co ₂ FeSn	4.24	5.70	4.22	4.69	0.56	Rh ₂ CoGa	4.24	3.00	4.26	2.41	0.81
Mn ₂ NiSn	4.36	0.00	4.35	0.52	0.40	Fe ₂ NiSn	4.25	4.63	4.26	5.22	0.58	Co ₂ NiSn	4.20	2.54	4.21	2.63	-0.03	Rh ₂ MnIn	4.44	4.29	4.47	4.22	1.30
Mn ₂ CuSn	4.42	6.64	4.41	0.52	0.27	Fe ₂ CuSn	4.30	4.36	4.30	4.68	0.31	Co ₂ CuSn	4.20	0.17	4.25	2.64	-0.34	Rh ₂ FeIn	4.42	4.24	4.43	3.45	1.09
Mn ₂ FeSb	4.26	6.35	4.23	3.00	0.31	Fe ₂ MnSb	4.20	4.05	4.26	6.52	0.22	Co ₂ MnSb	4.25	6.00	4.24	5.00	0.97	Rh ₂ CoIn	4.40	3.01	4.40	2.54	0.54
Mn ₂ CoSb	4.34	7.57	4.23	4.00	0.59	Fe ₂ CoSb	4.22	5.22	4.23	5.87	0.54	Co ₂ FeSb	4.22	5.35	4.20	4.27	0.22	Rh ₂ MnGe	4.29	4.73	4.32	3.12	1.43
Mn ₂ NiSb	4.35	0.00	4.34	0.67	0.36	Fe ₂ NiSb	4.22	4.16	4.26	5.04	0.29	Co ₂ NiSb	4.18	1.84	4.20	2.43	-0.15	Rh ₂ FeGe	4.28	3.54	4.28	2.87	0.88
Mn ₂ CuSb	4.42	6.48	4.40	1.07	0.08	Fe ₂ CuSb	4.27	3.86	4.29	4.26	0.07	Co ₂ CuSb	4.19	0.63	4.26	2.48	-0.69	Rh ₂ CoGe	4.25	2.33	4.26	2.23	0.71
Mn ₂ MoGa	4.17	-1.00	4.28	5.00	0.42	Fe ₂ MoGa	4.14	0.87	4.21	3.58	0.29	Co ₂ MoGa	4.17	2.89	4.16	0.78	0.55	Rh ₂ MnSn	4.45	4.76	4.47	3.71	1.41
Mn ₂ RuGa	4.29	7.15	4.21	1.02	0.73	Fe ₂ RuGa	4.19	5.55	4.19	5.47	0.60	Co ₂ MnGe	4.15	4.27	4.14	3.80	-0.16	Rh ₂ FeSn	4.42	3.54	4.42	3.04	0.85
Mn ₂ RhGa	4.33	7.80	4.23	1.68	0.62	Fe ₂ RhGa	4.20	0.00	4.18	5.04	0.80	Co ₂ RhGa	4.15	3.30	4.14	3.34	0.40	Rh ₂ CoSn	4.40	2.34	4.40	2.30	0.53
Mn ₂ PdGa	4.35	0.00	4.33	0.55	0.32	Fe ₂ PdGa	4.25	0.00	4.22	4.94	0.71	Co ₂ PdGa	4.18	2.67	4.18	3.03	0.17	Rh ₂ MnSb	4.45	4.67	4.46	3.43	1.05
Mn ₂ MoIn	4.33	-1.01	4.47	5.00	0.24	Fe ₂ MoIn	4.30	1.00	4.40	3.73	0.40	Co ₂ MoIn	4.33	2.99	4.32	0.67	1.07	Rh ₂ FeSb	4.44	3.18	4.41	2.59	0.44
Mn ₂ RuIn	4.45	7.63	4.41	1.02	0.31	Fe ₂ RuIn	4.36	6.18	4.36	5.81	0.31	Co ₂ RuIn	4.31	4.52	4.32	3.95	0.21	Rh ₂ CoSb	4.38	1.61	4.40	1.78	0.38
Mn ₂ RhIn	4.48	7.99	4.44	0.88	0.35	Fe ₂ RhIn	4.37	0.00	4.36	5.34	0.61	Co ₂ RhIn	4.31	3.41	4.32	3.51	0.16	Pd ₂ MnGa	4.38	4.08	4.40	3.77	0.64
Mn ₂ PdIn	4.52	0.00	4.50	0.38	0.28	Fe ₂ PdIn	4.41	5.27	4.40	5.20	0.63	Co ₂ PdIn	4.33	2.80	4.35	3.13	0.11	Pd ₂ FeGa	4.35	3.13	4.34	2.76	0.39
Mn ₂ MoGe	4.15	0.00	4.26	0.08	0.26	Fe ₂ MoGe	4.15	1.85	4.20	3.41	0.00	Co ₂ MoGe	4.18	3.51	4.16	0.23	-0.12	Pd ₂ CoGa	4.30	1.67	4.31	1.50	0.25
Mn ₂ RuGe	4.28	7.29	4.17	2.00	1.12	Fe ₂ RuGe	4.16	4.88	4.16	4.97	0.88	Co ₂ RuGe	4.15	4.02	4.13	3.19	-0.58	Pd ₂ MnIn	4.54	4.19	4.54	3.93	0.63
Mn ₂ RhGe	4.32	7.49	4.18	3.00	0.70	Fe ₂ RhGe	4.20	0.00	4.18	4.98	0.80	Co ₂ RhGe	4.15	3.09	4.15	3.34	0.34	Pd ₂ FeIn	4.50	3.18	4.48	2.86	0.39
Mn ₂ PdGe	4.35	0.00	4.33	0.57	0.14	Fe ₂ PdGe	4.23	4.65	4.24	5.25	0.41	Co ₂ PdGe	4.17	2.52	4.18	2.75	-0.11	Pd ₂ CoIn	4.46	1.74	4.46	1.59	0.17
Mn ₂ MoSn	4.31	0.00	4.45	0.04	0.23	Fe ₂ MoSn	4.31	2.12	4.40	3.96	0.34	Co ₂ MoSn	4.33	3.94	4.31	0.20	0.62	Pd ₂ MnGe	4.40	4.11	4.40	3.63	0.43
Mn ₂ RuSn	4.45	7.83	4.38	1.73	0.59	Fe ₂ RuSn	4.34	5.73	4.34	5.21	0.61	Co ₂ RuSn	4.30	4.10	4.30	3.32	-0.17	Pd ₂ FeGe	4.36	2.24	4.35	2.84	0.11
Mn ₂ RhSn	4.48	7.81	4.44	0.52	0.58	Fe ₂ RhSn	4.36	0.00	4.35	5.15	0.76	Co ₂ RhSn	4.30	3.05	4.32	3.38	0.16	Pd ₂ CoGe	4.32	1.64	4.31	1.31	0.02
Mn ₂ PdSn	4.51	0.00	4.50	0.43	0.24	Fe ₂ PdSn	4.39	4.84	4.40	5.29	0.48	Co ₂ PdSn	4.32	2.50	4.36	2.87	-0.09	Pd ₂ MnSn	4.54	4.14	4.54	3.75	0.56
Mn ₂ MoSb	4.30	0.00	4.41	1.00	-0.22	Fe ₂ MoSb	4.31	2.85	4.38	4.15	0.05	Co ₂ MoSb	4.32	0.00	4.32	0.00	0.07	Pd ₂ FeSn	4.51	3.21	4.49	2.84	0.21
Mn ₂ RuSb	4.43	7.51	4.33	3.00	0.87	Fe ₂ RuSb	4.31	5.01	4.33	4.95	0.75	Co ₂ RuSb	4.29	3.66	4.30	3.21	-0.49	Pd ₂ CoSn	4.46	1.65	4.45	1.25	0.01
Mn ₂ RhSb	4.46	0.00	4.44	0.51	0.46	Fe ₂ RhSb	4.33	4.59	4.35	5.50	0.62	Co ₂ RhSb	4.29	2.70	4.31	3.26	0.08	Pd ₂ MnSb	4.58	4.30	4.56	3.79	0.41
Mn ₂ PdSb	4.52	0.00	4.52	0.61	0.10	Fe ₂ PdSb	4.38	4.63	4.43	5.53	0.15	Co ₂ PdSb	4.31	2.06	4.35	2.71	-0.29	Pd ₂ FeSb	4.54	3.40	4.50	2.89	0.00
Mn ₂ WGa	4.18	-0.95	4.29	5.00	0.84	Fe ₂ WGa	4.15	0.94	4.22	3.51	0.72	Co ₂ WGa	4.16	1.72	4.17	0.69	0.79	Pd ₂ CoSb	4.48	1.81	4.45	1.08	-0.17
Mn ₂ OsGa	4.29	6.87	4.21	1.00	0.75	Fe ₂ OsGa	4.19	0.09	4.20	5.12	0.42	Co ₂ OsGa	4.16	4.08	4.16	3.58	-0.02	Ni ₂ MnAl	4.09	4.02	4.08	3.11	0.59
Mn ₂ IrGa	4.33	7.73	4.21	2.00	0.65	Fe ₂ IrGa	4.21	0.00	4.20	5.13	0.64	Co ₂ IrGa	4.17	3.50	4.16	3.40	0.35	Ni ₂ FeAl	4.06	3.17	4.04	2.79	0.19
Mn ₂ PtGa	4.36</																						

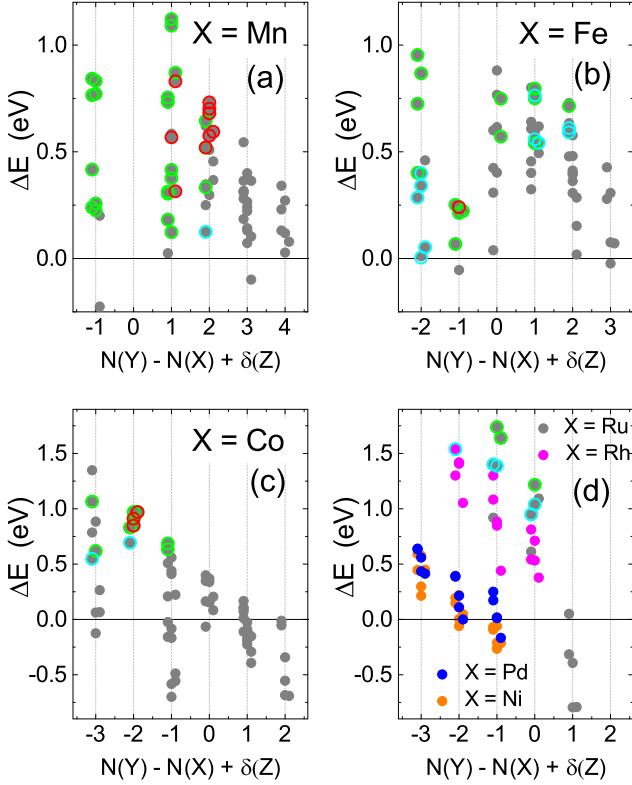


FIG. 2: (Color online). ΔE for X_2YZ compounds with $X=\text{Mn}$ (a), Fe (b), Co (c), and $X=\text{Ru,Rh,Pd,Ni}$ (d), see text for details.

culations for a subset of 259 compounds from among the X_2YZ Heuslers with $X=\{\text{Mn,Fe,Co,Ni,Ru,Rh,Pd}\}$, $Y=\{\text{Mn,Fe,Co,Ni,Cu,Mo,Ru,Rh,Pd,W,Os,Ir,Pt}\}$, and $Z=\{\text{Al,Ga,In,Si,Ge,Sn,Sb}\}$ using the VASP program¹⁶ with PAW potentials and PBE GGA/DFT functional^{17,18}. In Table I we show the calculated lattice constants and magnetic moments of regular and inverse phases and the total energy difference, ΔE , between the phase where the lower-valence (or lower atomic number if valence is the same) atom does not and where it does occupy site II for all considered compounds. Note that ΔE is positive if the 'lightest atom' rule is satisfied. The convergence of these results was verified by varying the number of divisions in reciprocal space from $10 \times 10 \times 10$ to $18 \times 18 \times 18$ and the energy cut-off from 400 eV to 520 eV. In Supplemental Material we show the figures of DOS and minority bands of these compounds.

Fig 2 shows ΔE for 259 compounds as a function of $N(Y) - N(X) + \delta(Z)$, where we define $\delta(Z) = 0.1[N(Z) - 4]$, for illustrative purposes: compounds with $N(Z)=3,4,5$ are displayed with slight shifts from the guide-lines. The 'lightest atom' rule is valid ($\Delta E > 0$) for 66 out of the 68 Mn_2YZ compounds considered and 62 out of the 64 Fe_2YZ compounds considered. $\Delta E > 0$ for all Co_2YZ ($Y=\text{Mo,W,Mn}$), Ru_2YZ ($Y=\text{Mn,Fe}$), Rh_2YZ ($Y=\text{Mn,Fe,Co}$), Pd_2YZ ($Y=\text{Mn,Fe}$),

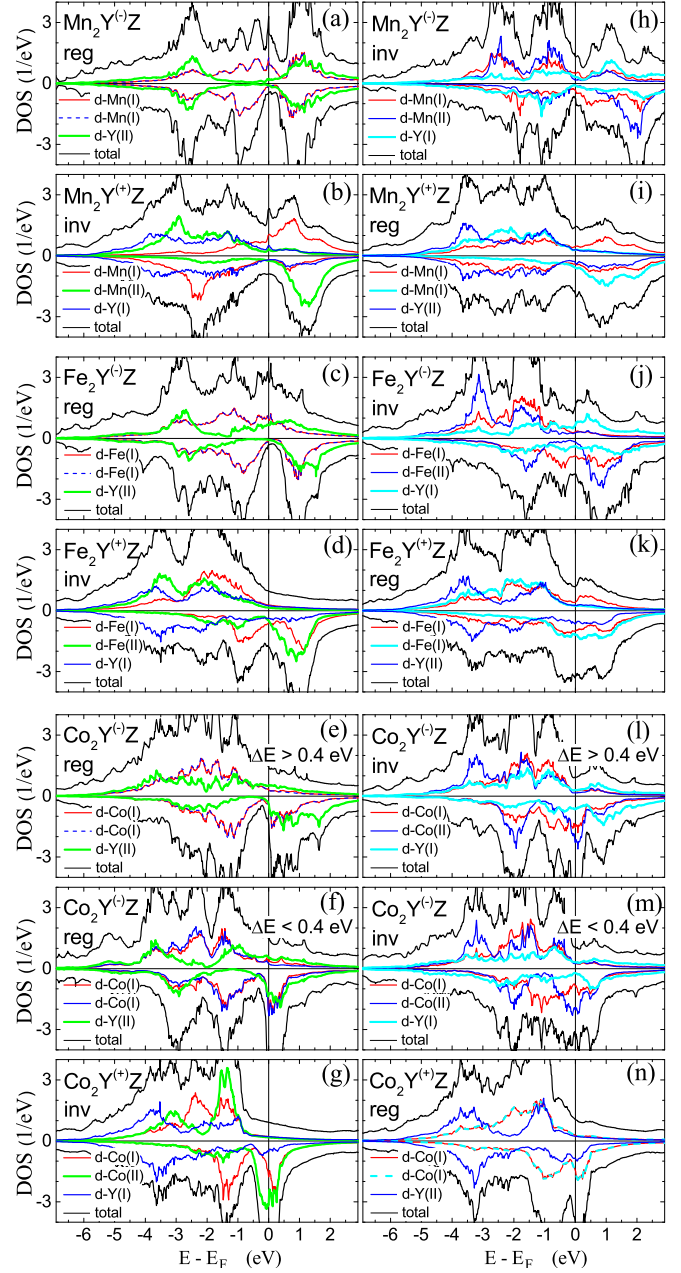


FIG. 3: (Color online). (a-g) DOS averaged over Z and $Y^{(\pm)}$ for sets of $X_2Y^{(\pm)}Z$ compounds where $X=\text{Mn,Fe,Co}$ for phases that satisfy the 'lightest atom' rule. (h-n) same as (a-g) for the corresponding phase that does not satisfy the 'lightest atom' rule.

and Ni_2MnZ compounds considered (except Co_2MoGe). As discussed above the 'lightest atom' rule cannot reliably predict the stable phase of compounds when $N(X)$ and/or $N(Y)$ is too large. Therefore ΔE typically reduces when $N(Y)$ increases [as seen on Fig. 2 (c),(d) this trend is especially well pronounced for heavier $X=\text{Co,Ni,Ru,Rh,Pd}$] and many compounds in heavier subsets: Co_2YZ ($Y=\text{Fe,Ni,Cu,Ru,Rh,Pd,Os,Ir,Pt}$), Ru_2CoZ , Pd_2CoZ , Ni_2YZ ($Y=\text{Fe,Co}$) have $\Delta E < 0$.

In Fig 2 the half-metallic compounds ($dM = 0$) are indicated by red open circle, compounds with $0 < dM \leq 0.06$ and $0.06 < dM \leq 0.15$ are indicated by green and cyan open circle, correspondingly. Here $dM \equiv |M_t - (N_t - 24)|$ measures the validity of the Slater-Pauling rule. Many light Heuslers: Mn_2YZ and Fe_2YZ [$N(Y) - N(X) \leq 2$], Co_2YZ [$Y=Mo,W,Mn$] and Ru_2YZ [$Y=Mn,Fe$] have Slater-Pauling behaviour. Compounds with smaller dM typically have higher ΔE since both, higher ΔE and Slater-Pauling behavior (and half-metallicity), originates from E_F being within the SP valley.

Fig 3(a-g) show the DOS for $X_2Y^{(\pm)}Z$ compounds with $X=Mn,Fe,Co$, averaged over all considered in present work Z and $Y^{(\pm)}$, where the phase is chosen in agreement with the 'lightest atom' rule: regular for $Y^{(-)}$ with $N(Y^{(-)}) < N(X)$, and inverse for $Y^{(+)}$ with $N(Y^{(+)}) \geq N(X)$. [Number of averaged compounds can be deduced either from Fig 2 or from Table I]. For $Co_2Y^{(-)}Z$ compounds where E_F is very close to the higher edge of the SP valley we additionally separated compounds to that with $\Delta E > 0.4eV$ and that with $\Delta E < 0.4eV$ [see Fig 2 (e),(g)].

The SP valley between (11r/i) and (12r/i) bands is clearly seen in Fig 3(a-g) as the valley near E_F in red-colored and blue-colored pDOS of atoms on site I and site I', correspondingly. For inverse $X_2Y^{(+)}Z$ compounds with $X=Fe,Co$ the SP valley is formed mostly by Fe or Co pDOS (red) since pDOS of heavy $Y^{(+)}$ (blue) is small near E_F (most of the DOS structure of these heavy atoms is located far below E_F). Since it is energetically favorable, E_F is often located within the SP valley, although for heavier Co_2YZ , E_F shifts to the higher edge of the SP valley.

Due to non-bonding of states (9-13r/i) to site II the minority pDOS of the (lower-valence) atom on site II [green lines in Fig 3(a-g)] have a wide valley. E_F is located lower than the higher energy edge of this valley [determined mostly by state (15r/i)] for $X=Mn,Fe$, right on the edge for $Co_2Y^{(-)}Z$ with $\Delta E > 0.4eV$, slightly above the edge for $Co_2Y^{(-)}Z$ with $\Delta E < 0.4eV$, and far above the edge for $Co_2Y^{(+)}Z$. As discussed above, peaky DOS structure at E_F in last two cases leads to violations of the 'lightest atom' rule: Fig 2(c) shows many points with $\Delta E < 0$ for Co_2YZ compounds with $N(Y) - N(X) \geq -1$.

Fig 3(h-n) show averaged DOS for the same compounds as Fig 3(a-g), but with different phase - when lower-valence atom is switched from site II to site I'. Due to this switch, the energy of the bands mostly localized on site II decreases and the energy of bands mostly localized on sites I and I' increases, so the SP valley closes and the minority DOS increases near E_F in Fig 3 (h-l) and near $E_F - 0.5 eV$ in Fig 3(m,n), as compared to the DOS in corresponding Fig. 3(a-g). The described above behavior of the DOS averaged over broad classes of compounds (as well as DOS of individual compounds presented in Supplemental Material) confirm that the 'lightest atom' rule indeed originates from the increase of the total en-

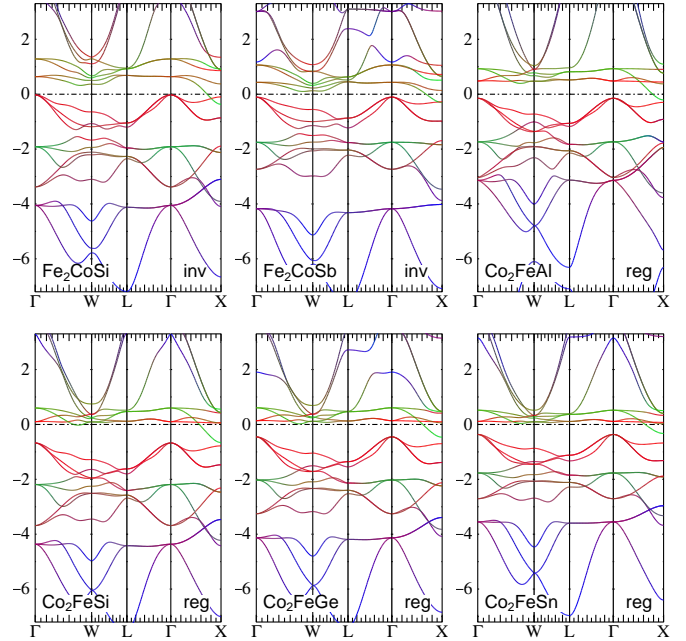


FIG. 4: Minority bands of the stable phase (inverse for $X=Fe$ and regular for $X=Co$) of 6 Heusler compounds that are not half-metallic *exclusively* due to the drop of a (green) band that includes the (15r/i) state at the X-point below the Fermi energy.

ergy due to increase of the minority DOS at E_F when lower-valence atom is switched from site II to site I' (or I).

IV. HALF-METALLICITY RULE

A. Half-metallicity rule for compounds with $M_t = N_t - 24$ Slater-Pauling behaviour

We found that in all considered cases where the SP valley exists near E_F and site II is occupied by a higher-valence atom than Mn, the energy of state (15r/i) at X-point drops below the energy of states (ix,x,xi) at Γ -point and/or below E_F . Examples of such behaviour can be seen in Fig. 4 that shows minority bands of Fe_2CoSi , Fe_2CoSb , Co_2FeAl , Co_2FeSi , Co_2FeGe , and Co_2FeSn compounds. One can see that the band gap of these compounds is closed exclusively due to the drop of the energy of the state (15r/i) at the X-point below the Fermi energy. This drop in energy can be explained by the fact that the wavefunction of the state (15r/i) is localized on site II which is occupied by 'too heavy' atom (atom with valence higher than valence of Mn) which drags the energy of the state (15r/i) below E_F . Therefore, in all these cases there is no minority band-gap at E_F .

On the other hand, if a lower-valence atom than Mn occupies site I or I', then, according to the 'lightest atom' rule, site II should be occupied by an atom with equal

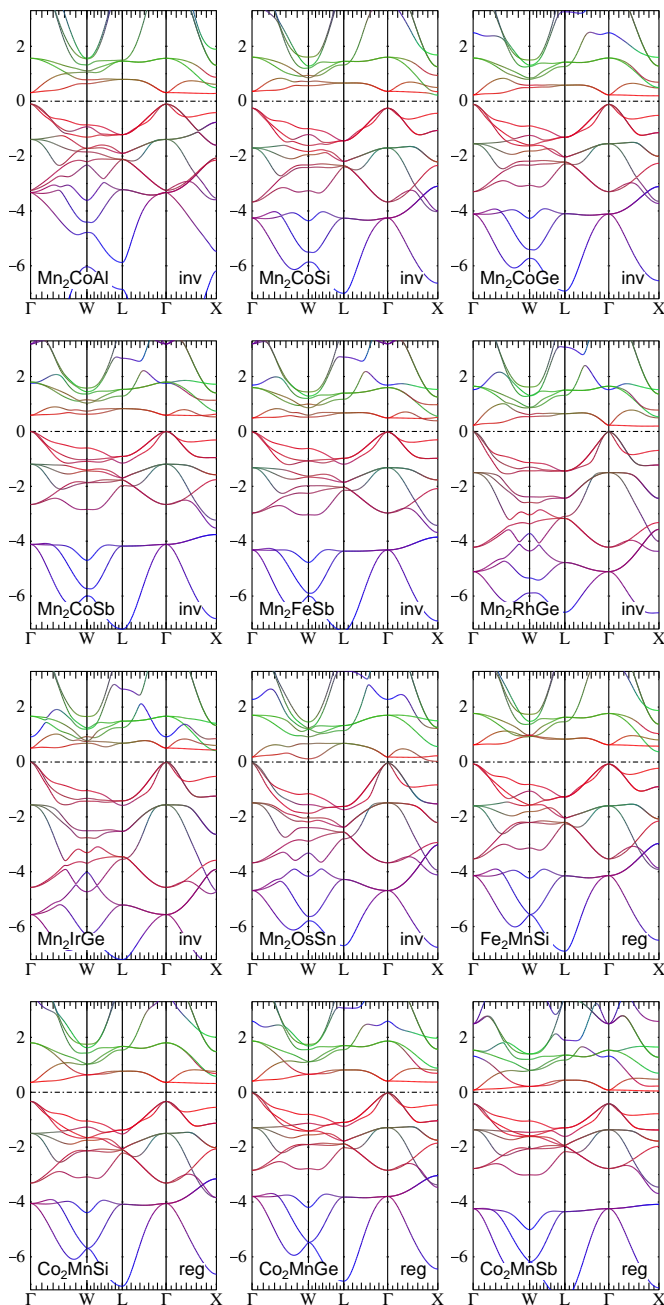


FIG. 5: Minority bands of the stable phase (inverse for X=Mn and regular for X=Fe,Co) of 12 half-metallic Heusler compounds that have the Slater-Pauling behaviour.

or still lower-valence, thereby resulting in states (ix,x,xi) lying above E_F , so again there is no minority band-gap at E_F [exception from this statement will be considered in section C below]. Therefore, we can formulate the 'half-metallicity' rule: "The half-metallic cubic Heusler compound should have an atom on site II with the same or lower valence than Mn, and atoms on sites I and I' with the same or higher valence than Mn".

Fig. 5 shows the minority band structure of 12 half-

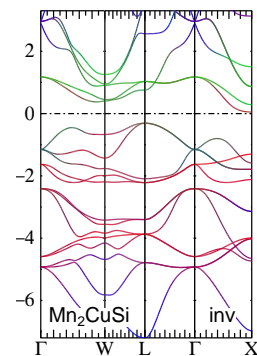


FIG. 6: Minority bands of the half-metallic inverse phase of Mn_2CuSi .

metallic Heusler compounds that have magnetic moment satisfying the $M_t = N_t - 24$ Slater-Pauling rule. In all these compounds site II is occupied by Mn atom and therefore the (green-colored) state (15r/i) at X-point has energy above E_F [compare to Fig 4]. Thus, the half-metallicity rule derived above is supported by our findings of half-metallicity only for Heusler compounds with Mn on site II and Mn,Fe,Co,Rh,Ir,Os on sites I and I'.

Several dozens of regular and inverse cubic Heusler compounds that are predicted by DFT calculations to be half-metallic with $M_t = N_t - 24$ Slater-Pauling magnetic moment can be found in literature (see, e.g.^{8,14,19}). To the best of our knowledge, all these half-metallic Heusler compounds satisfy our half-metallicity rule without a single exception.

B. Half-metallicity rule for compounds with generalized $M_t = N_t - 28$ Slater-Pauling behaviour

On Fig. 6 we show the minority band structure of half-metallic inverse Mn_2CuSi (inverse phase is 0.03 eV lower in energy compared to regular phase of this compound, see Table I). This compound is the only half-metallic compound found among considered in present work compounds that does not have the $M_t = N_t - 24$ Slater-Pauling behavior. Magnetic moment of Mn_2CuSi is $1.0\mu_B$ (see Table I) while the $M_t = N_t - 24$ Slater-Pauling rule predicts the magnetic moment of $5.0\mu_B$ for this compounds. The Slater-Pauling behaviour is violated in this compounds since two bands that include states (xii,xiii) at the Γ -point [these states are localized on sites I and I'] are dragged below E_F by heavy Cu that occupies site I (compare minority bands of Mn_2YSi within the series of Y=Fe,Co,Ni,Cu in Supplemental Material). The shift of two minority bands from fully unoccupied to fully occupied leads to reduction of the magnetic moment by $4\mu_B$.

Nevertheless, according to the half-metallicity rule derived above, inverse Mn_2CuSi is still allowed to be half-metallic since site II is occupied by light Mn atom and, therefore, localized on site II state (15i) can have energy

above E_F . This is indeed what one can see on Fig. 6 - state (15i) at the X -point has energy $E_F + 0.25$ eV and the band gap is not closed by the (green) band that includes this state (compare with closure of the gap in compounds shown in Fig. 4).

Inverse Mn_2CuSi is one of several known in literature half-metallic compounds that satisfy the so-called generalized $M_t = N_t - 28$ Slater-Pauling rule for inverse Heusler compounds¹⁴. Other known members of this class of half-metallic compounds include inverse Cr_2ZnSi and Mn_2ZnSi . As one can see these two compounds also satisfy our half-metallicity rule. Since switch of the $M_t = N_t - 24$ behavior to $M_t = N_t - 28$ behavior is due to the high valence of the atom on site I, the energy of the (15i) state which is localized on site II should not be affected much by this change of the Slater-Pauling behavior and, therefore, the half-metallicity rule derived above should still work for compounds with $M_t = N_t - 28$ behavior.

C. C. Half-metallicity rule for compounds with generalized $M_t = N_t - 18$ Slater-Pauling behaviour

Another class of inverse half-metallic compounds known in literature satisfy the generalized $M_t = N_t - 18$ Slater-Pauling rule¹⁴. Known members of this class include inverse compounds: Sc_2CrAl , Sc_2MnAl , Sc_2VSi , Sc_2CrSi , Sc_2MnSi , Sc_2CoSi , Ti_2MnAl , Ti_2FeAl , Ti_2CoAl , Ti_2NiAl , Ti_2VSi , Ti_2FeSi , Ti_2CoSi , Ti_2VAs , V_3Al , V_2CrAl , V_2MnAl ¹⁴, Ti_2CoB ²⁰, and Ti_2CoGa ²¹.

The change from $M_t = N_t - 24$ behavior to $M_t = N_t - 18$ behavior in these compounds originates from presence of the low valence atoms X on sites II and I' that pushes three bands that include states (ix,x,xi) at the Γ -point from below E_F to above E_F . The shift of three minority bands from fully occupied to fully unoccupied leads to increase of the magnetic moment by $6 \mu_B$.

Since states (ix,x,xi) at the Γ -point have energy above E_F the half-metallicity rule derived in section A for compounds that satisfy the $M_t = N_t - 24$ rule should be modified for compounds that satisfy the $M_t = N_t - 18$ rule and include only one condition. Thus, the modified (less restrictive) rule for this class of compounds reads: "The half-metallic inverse cubic Heusler compound that satisfy generalized $M_t = N_t - 18$ Slater-Pauling rule should have an atom on site II with the same or lower valence than Mn". To the best of our knowledge all half-metallic compounds with $M_t = N_t - 18$ behavior satisfy this modified half-metallicity rule without single exception.

V. V. GENERAL TRENDS IN MAGNETIC STRUCTURE OF CUBIC HEUSLER COMPOUNDS

As seen in Table I (and also in Fig 3) the X_2YZ compounds with $\text{X}=\text{Mn,Fe,Co,Ru,Rh}$ typically have mag-

netic moment that satisfies the $M_t = N_t - 24$ Slater-Pauling rule (exactly or approximately) at the low-valence end of corresponding Y-series. When valence of the Y atom increases the SP valley in minority DOS moves to lower energies from E_F (or even closes) and minority bands are filled by more than 12 electrons. Thus, the magnetic moment reduces as compared to the $N_t - 24$ prediction. As seen from corresponding DOS figures (DOS and minority bands figures are presented for all considered compounds in Supplemental Material) the SP valley for heavier compounds with $\text{X}=\text{Pt,Ni}$ is always located below E_F , so the magnetic moments of these compounds are always less than $N_t - 24$ (see Table I).

Compounds with $\text{X}=\text{Mn}$ and Y atoms with valence higher than Mn ($\text{Y}=\text{Fe,Co,Ni}$, etc) typically have antiferromagnetically (AFM) coupled Mn atoms in stable inverse phase (this phase satisfies the 'lightest atom' rule) with large absolute values of magnetic moment ($> 2.5\mu_B$) on Mn atoms. One reason for this is that in many Mn_2YZ compounds that have (energetically favourable) Slater-Pauling behavior generally small values of $N_t - 24$ (as compared to compounds with $\text{X}=\text{Fe,Co}$ and similar Y and Z) make the AFM coupling of two Mn atoms preferred over the FM coupling in inverse phase. Compounds with $\text{X}=\text{Mn}$ and Y atoms with valence lower than Mn ($\text{Y}=\text{Mo}$ or W) either have ferromagnetically (FM) coupled Mn atoms with low ($< 1\mu_B$) magnetic moments on Mn atoms (Mn_2MoGa , Mn_2MoIn , Mn_2WGa , Mn_2WIn , and Mn_2WSb) or are non-magnetic (Mn_2MoGe , Mn_2MoSn , Mn_2WGa , and Mn_2WIn) in stable regular phase (this phase satisfies the 'lightest atom' rule) with a single exception of Mn_2MoSb that has inverse stable phase.

Compounds with $\text{X}=\text{Fe,Co,Ni}$ typically have two FM coupled magnetic X atoms. The FM coupling is energetically favorable for these materials since, unlike the complex AFM structure of bulk Mn, parent bulk materials Fe,Co, or Ni have FM coupling. Also, parent bulk Fe, Co, and Ni metals have lower absolute value of the magnetic moment per atom as compared to the magnetic moment of Mn atoms in bulk Mn, while Heusler compounds with $\text{X}=\text{Fe,Co,Ni}$ have larger $N_t - 24$ as compared to $N_t - 24$ of X_2YZ compounds with $\text{X}=\text{Mn}$ and the same Y and Z atoms. Therefore, for Heusler compounds with $\text{X}=\text{Fe,Co,Ni}$ that have (energetically favourable) Slater-Pauling behavior, larger values of $N_t - 24$ make the FM coupling of two X atoms preferred over the AFM coupling in both regular and inverse phase.

VI. VI. CONCLUSION

In conclusion, we developed an 18-orbital coupling model for cubic full Heusler compounds that explain the orbital composition, symmetry and energy ordering of 18 states near E_F at the Γ and X symmetry points. We show that due to the high symmetry of the regular Heusler compound each of 18 considered states at the Γ and X symmetry points are composed from no more than

two orbitals from the list of 18 orbitals that significantly simplifies analysis of the system. Based on this analysis we derived a *unified* set of rules for Heusler compounds that accounts for their chemical ordering ('lightest atom' rule), their magnetic moment (Slater-Pauling rule), and those compositions most likely to be half-metallic (half-metallicity rule). The limitation of the 'lightest atom' rule is that it cannot be applied to heavy compounds. To the best of our knowledge all known in literature half-metallic Heusler compounds that follow the $M_t = N_t - 24$ or $M_t = N_t - 28$ Slater-Pauling behaviour satisfy the half-metallicity rule without a single exception. DFT calculations performed for 259 compounds confirm the validity

of our model and derived rules for broad classes of Heusler compounds.

VII. ACKNOWLEDGEMENT

S.F. acknowledges the CNMS User support by Oak Ridge National Laboratory Division of Scientific User facilities. S.F. thanks Oleg Mryasov for useful discussions and Elena Faleeva for preparing the picture of Heusler structure.

* Electronic address: svfaleev@us.ibm.com

† Electronic address: stuart.parkin@mpi-halle.mpg.de

¹ T. Graf, C. Felser, and S. S. P. Parkin, *Prog. Solid State Chem.* **39**, 1 (2011).

² C. Felser, G. H. Fecher, and B. Balke, *Angew. Chem.* **119**, 680 (2007).

³ R. Kainuma *et al.* *Nature* **439**, 957 (2006).

⁴ S. Chadov, X. Qi, J. Kübler, G. H. Fecher, C. Felser, S. C. Zhang, *Nat. Mater.* **9**, 541 (2010).

⁵ M. Franz, *Nat. Mater.* **9**, 536 (2010).

⁶ M. Jourdan *et al.* *Nature Comm.* **5**, 3974 (2014).

⁷ Liu, H.-x. *et al.* *Appl. Phys. Lett.* **101**, 132418 (2012).

⁸ H. C. Kandpal, G. H. Fecher, and C. Felser, *J. Phys. D: Appl. Phys.* **40**, 1507 (2007).

⁹ H. Luo *et al.*, *J. Phys. D: Appl. Phys.* **41**, 055010 (2008).

¹⁰ L. Wollmann, S. Chadov, J. Kübler, and C. Felser, *Phys. Rev. B* **90**, 214420 (2014).

¹¹ I. Galanakis, P. H. Dederichs, and N. Papanikolaou, *Phys. Rev. B* **66**, 174429 (2002).

¹² G. D. Liu *et al.*, *Phys. Rev. B* **77**, 014424 (2008).

¹³ J. Kübler, *Physica B+C* **127**, 257 (1984).

¹⁴ S. Skaftouros, K. Özdoğan, E. Şaşıoğlu, and I. Galanakis, *Phys. Rev. B* **87**, 024421 (2013).

¹⁵ S. V. Faleev, Y. Ferrante, J. Jeong, M. G. Samant, B. Jones, and S. S. P. Parkin, submitted to *Phys. Rev. Appl.* (2016).

¹⁶ G. Kresse and J. Furthmüller, *Phys. Rev. B* **54**, 11169 (1996).

¹⁷ P. E. Blochl,

¹⁸ G. Kresse and D. Joubert, *Phys. Rev. B* **59**, 1758 (1999).

¹⁹ I. Galanakis, in *Heusler Alloys*, edited by C. Felser and A. Hirohata, Springer Series in Materials Science **222** (Springer International Publishing, Switzerland, 2016).

²⁰ N. Kervan, S. Kervan, *Solid State Commun.* **151**, 1162 (2011).

²¹ N. Kervan, S. Kervan, *J. Magn. Magn. Mater.* **324**, 645 (2012).